DOI: 10.1002/chem.200702032

Self-Assembly of Two Different Hierarchical Nanostructures on Either Side of an Organic Supramolecular Film in One Step

Naien Shi,[a] Gui Yin,[a] Min Han,[a] Lei Jiang,[b] and Zheng Xu*[a]

Abstract: We fabricated different hierarchical organic nanostructures on each side of a supramolecular film, by using hydrogen-bonding interactions between tetrapyridylporphyrin and benzene-1,3,5-tricarboxylic acid at the H_2O/$CHCl_3$ interface. The surface of the film that faces water is composed of nanoprism arrays, whereas the surface facing $CHCl_3$ is composed of three-dimensional sunflower-like hierarchical micro- and nanostructures. FTIR spectral evidence showed that all pyridyl groups of the tetrapyridylporphyrin hydrogen bonded to the carboxylic acid groups of 1,3,5-benzene-tricarboxylic acid. The aggregation modes of porphyrin presented in this supramolecular film were studied by UV/Vis and fluorescence spectroscopy. Moreover, each side of the film exhibits distinct soakage properties.

Keywords: hierarchical interface · hydrogen bonds · organic nanostructures · self-assembly · supramolecular films

Introduction

Self-assembled structures with highly specific morphology and properties are of intense interest to chemists and materials scientists.[1] Assembling the synthesized nanoscale building blocks into advanced structures is a necessary approach for applications in integrated devices. Extensive research has been devoted to the development of synthetic strategies for highly organized building blocks, such as monolayer-protected nanoparticles,[2–4] aggregation-based growth of nanoparticles,[1] or in-situ assembly.[5] In comparison, progress towards organic nanostructures with advanced architecture lags far behind that of their inorganic counterparts, although a variety of organic nanostructures have been prepared, such as nanoparticles, nanorods, nanoribbons, or nanotubes.[6–9] There is, therefore, an intense interest in developing methods for preparing highly organized advanced architectures from self-assembling organic nanostructures.

Herein, we describe the successful fabrication of different three-dimensional hierarchical nanostructures on both sides of an organic supramolecular film. The film is formed from tetrapyridylporphyrin (TPyP) and 1,3,5-benzene-tricarboxylic acid (BTC). By taking advantage of the different solubilities of TPyP and BTC in water and $CHCl_3$, a two-phase $H_2O/CHCl_3$ system was designed for fabricating the supramolecular film. BTC in H_2O can encounter TPyP in $CHCl_3$ at the interface and form a supramolecular film by hydrogen bonding and π–π-stacking interactions. An ordered array of uniform nanoprisms was formed on the H_2O side, whereas a sunflower-like hierarchical micro- and nanostructure formed on the reverse side facing towards the $CHCl_3$ layer. This is of great value to fundamental studies in supramolecular self-assembly and for practical applications in nanotechnology. Typically, an aliquot of an aqueous solution of BTC

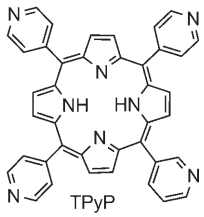

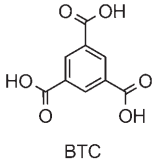

[a] Dr. N. Shi, Dr. G. Yin, Dr. M. Han, Prof. Z. Xu
State Key Laboratory of Coordination Chemistry
National Laboratory of Solid State Microstructures
School of Chemistry and Chemical Engineering
Nanjing University, Nanjing 210093 (P.R. China)
Fax: (+86) 25-8331-4502
E-mail: zhengxu@netra.nju.edu.cn

[b] Prof. L. Jiang
Center of Molecular Sciences
Institute of Chemistry, Chinese Academy of Sciences
National Center for Nanoscience and Technology
Beijing 100080 (P.R. China)

Supporting information for this article is available on the WWW under http://www.chemeurj.org/ or from the author.

(4 mM or 6 mM) was added to the $CHCl_3$ solution of TPyP (0.5 mM) at 25 °C (TPyP was synthesized according to the literature[10]). An interface between H_2O and $CHCl_3$ was formed immediately, and then a thin film that gradually thickened was formed at the interface. Simultaneously, the colour of the $CHCl_3$ phase slowly disappeared, which indicated that TPyP was transferred and combined into the film at the interface. After a given time, the film referred to as film I ([BTC] = 4 mM) or film II ([BTC] = 6 mM), was transferred and washed by distilled water to remove the adsorbed BTC. The film was characterized by SEM, ^{1}H NMR, FTIR, UV/Vis, and fluorescence spectroscopy measurements.

Results and Discussion

By using the interfacial assembly method, we obtained a TPyP–BTC two-component supramolecular film with distinct hierarchical structures on either side. For clarity, the surfaces facing towards the H_2O and $CHCl_3$ phases are abbreviated as film *X*-W and film *X*-O, respectively, in which *X* = I or II depending on the BTC concentration. For film I-W, the SEM image clearly shows that it is an ordered array of uniform nanoprisms (Figure 1a). The corresponding enlarged image shows that all the prisms are straight-standing with a sharp tip, approximately 300–500 nm in size (Figure 1b). The appearance of some imperfect prisms indicates that they may be composed of nanosheets. Interestingly, for film I-O a special three-dimensional hierarchical morphology is obtained, which consists of many flowerlike microtextures that are ≈5 to ≈50 μm in diameter (Figure 1c), growing on an irregular aggregate substrate (Figure 1e). The specified enlarged flower microtexture is just like the "sunflower" (Figure 1d). The petals of the microtexture are composed of irregular prisms, whereas the pistils are smaller nanoprisms similar to those of film I-W. To the best of our knowledge, this is the first report of three-dimensional highly organized hierarchical micro- and nanostructures assembled by two small organic molecules; furthermore, two distinct hierarchical structures are respectively assembled on either side of one film in one step. The hierarchical supramolecular film obtained is very stable, even when vigorously shaken. By simply controlling the area of the interface, a centimetre-scale film can easily be fabricated, which is beneficial for large-scale production.

In the FTIR spectra of film I (Figure 2a), the vibration band of the pyridyl rings at 1593 cm^{-1} disappeared and a pyridinium vibration band at 1628 cm^{-1} appeared, which indicates that all the pyridyl groups are strongly bonded to BTC by means of hydrogen bonding.[11,12] Moreover, the band at 2154 cm^{-1} arises from Fermi resonance between the

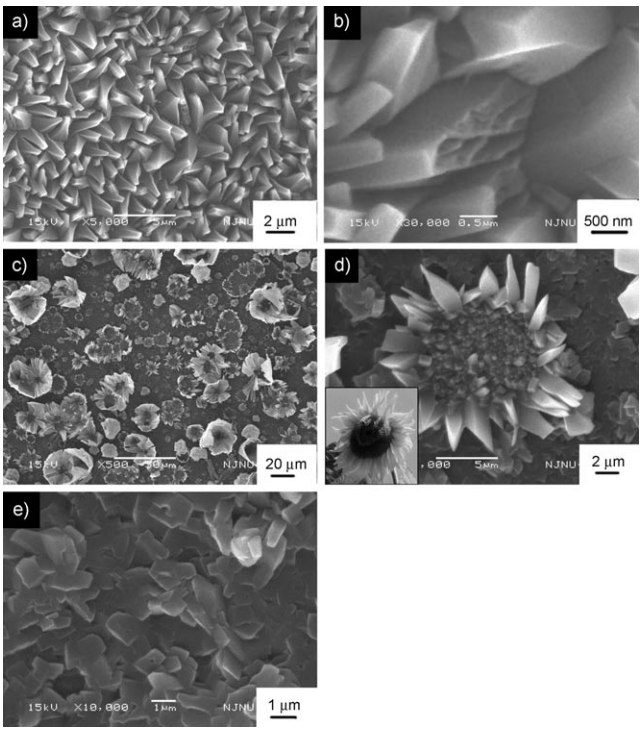

Figure 1. a) Low and b) high magnification of the SEM image of film I-W. c) SEM image of film I-O. d) SEM image of an enlarged sunflower-like microstructure. e) SEM image of a region beside the flower microtexture in c).

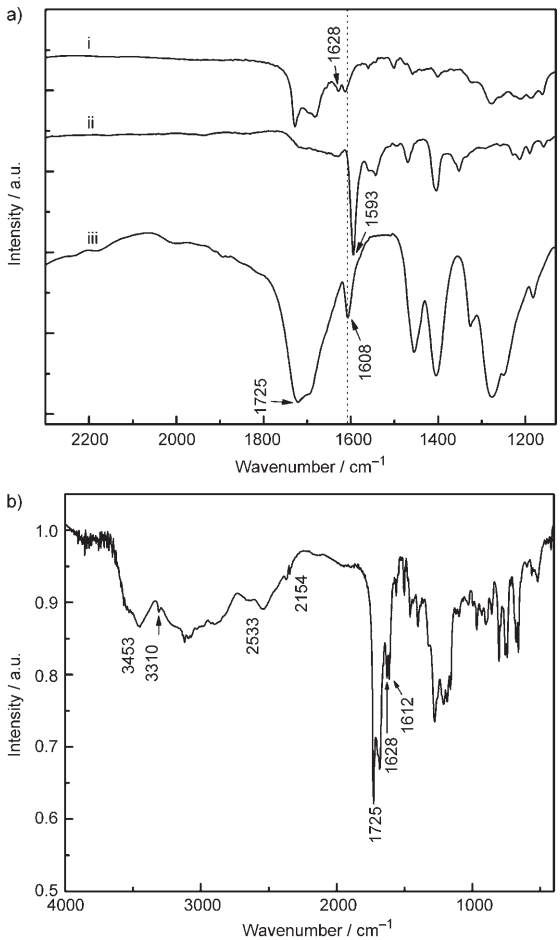

Figure 2. FTIR spectra of a) i) the film, ii) TPyP, and iii) BTC. b) The whole region of the film.

vibration of the O–H bond and the pyridyl rings,[12] which further confirms the presence of strong hydrogen bonds between these groups (Figure 2b). The composition of the film was determined by ^{1}H NMR spectroscopy. It must be noted that this film is not soluble in common solvents because solvation effects cannot overcome the intermolecular forces in the film. A proton source (CF_3COOH) was added to break the hydrogen bonds between TPyP and BTC to give a transparent [D_6]DMSO solution of the film, which was suitable for NMR spectroscopy. ^{1}H NMR spectroscopy results (see Figure S1 in the Supporting Information) confirmed that it is composed of TPyP and BTC with an average molar ratio of TpyP to BTC of 1:3, based on the ratio of the integral areas of signals for the protons in the methine ($\delta =$ 8.87 ppm, in TPyP) and phenyl ($\delta = 8.61$ ppm, in BTC) groups. A similar result was obtained for film II at 6 mM BTC.

To get an insight into the formation process of the film, a time-dependent experiment was conducted. Figure 3 shows the SEM images of film I-W formed at 10 min, 30 min, 3 h, and 16 h, respectively. As soon as the interface formed (10 min), a very thin film composed of many $\approx$80 nm particles was obtained. This was the primary nucleus that was transferred and investigated. After 30 min or so, the particles grew outward and became nanoribbons. This was followed by the aggregation of the nanoribbons, which stacked to form prism precursors after a 3 h reaction. Finally, perfect prisms were formed after a 16 h experiment. Whereas for film I-O (Figure 4a–d), a lot of procumbent irregular plates were formed at first (30 min), followed by the formation of big plates (16 h). There were only a few flowerlike hierarchical microstructures (3 days) and they gradually increased in number (6 days). Because the interface was disturbed during sample acquisition, the morphology of the final product obtained at 6 days (Figure 4d) was slightly different from that shown in Figure 1c. The film grew from the primary nucleus and in the end formed an integrated hierarchical structure.

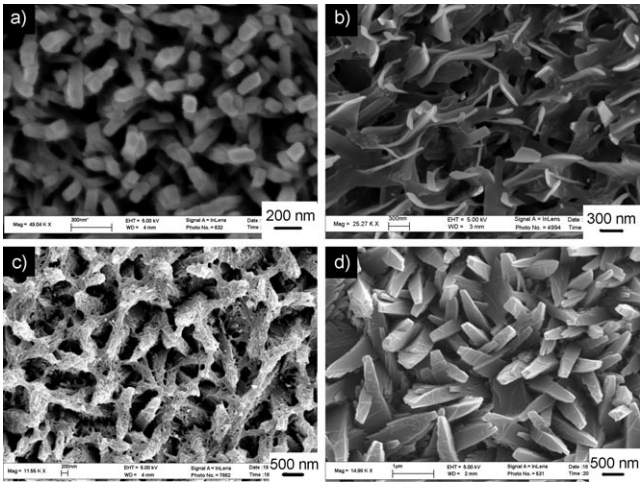

Figure 3. SEM images of the formation process for the H_2O face of film I after a) 10 min, b) 30 min, c) 3 h, and d) 16 h.

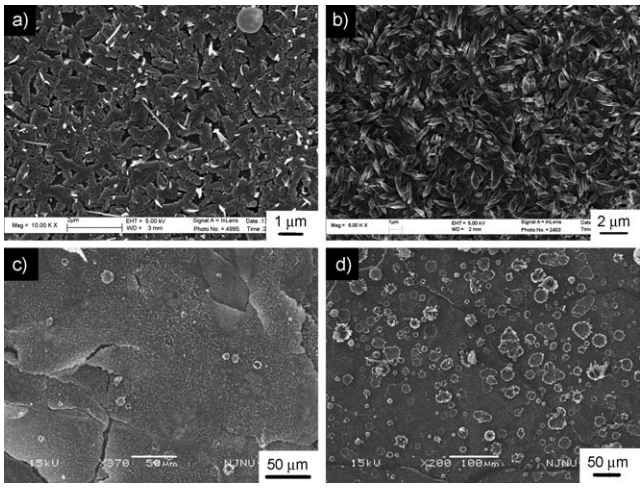

Figure 4. SEM images of the formation process for the $CHCl_3$ face of film I after a) 30 min, b) 16 h, c) 3 days, and d) 6 days.

Moreover, the concentration of BTC and the temperature have an obvious effect on the formation of the film. During the experiment, we found that the film grew faster when the concentration of BTC increased to 6 mM (film II). The corresponding SEM image (Figure 5a) showed that the obtained nanoprisms were smaller than in film I-W at 4 mM BTC. They were 100–200 nm in size because the rate of the nucleation accelerated as the BTC concentration increased. At the same time, on the reverse side of the supramolecular film, discrete microtextures for film I-O at 4 mM BTC became flower-in-flower compact structures for film II-O at 6 mM BTC (Figure 5b). When the temperature decreased from 25 to 18 °C, the sunflower petal structure was replaced by a bubblelike structure (Figures 5c,d). This implies that the formation of a flowerlike microstructure might correlate with the gas bubble that resulted from escaping $CHCl_3$. The supramolecular film covering the $CHCl_3$ phase prevents the

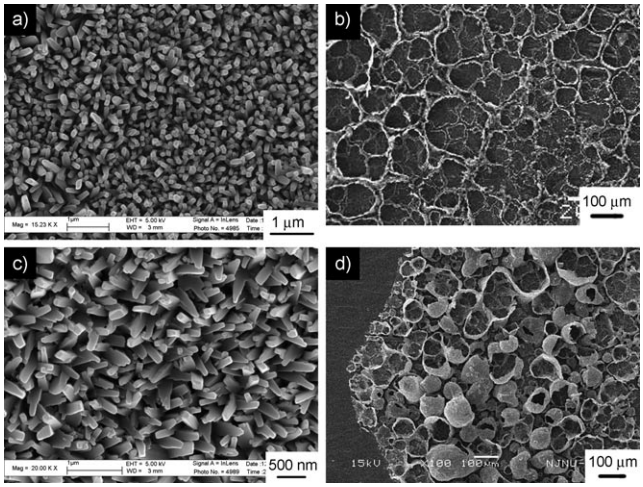

Figure 5. SEM images of a) film II-W and b) film II-O at 25 °C. SEM images of (c) film I-W and (d) film II-O at 18 °C (experimental conditions, BTC:6 mM, TPyP:0.5 mM).

gas from escaping from the solution and it tends to adhere on the rough surface of the film to form a small bubble. Because the gas formation process is slow, the primary bubbles are relatively small. After an extended time, some small primary bubbles slowly aggregate to form a large one. A lot of flower-in-flower compact structures on the side toward $CHCl_3$ provide evidence for the aggregation process (Figures 1c and 5b,d). In the bubble, there are two different areas, I (interior of the bubble) and II (border of the bubble). In area I, the supramolecular prism grows on the film substrate, whereas in area II, the prism grows at the periphery of the bubble. Although the concentration of BTC is identical in areas I and II, the concentration of TPyP is higher in area II than in I, which induces faster growth in area II than in I. As a result, longer petals are formed in area II and shorter pistils in area I (Figure 6).

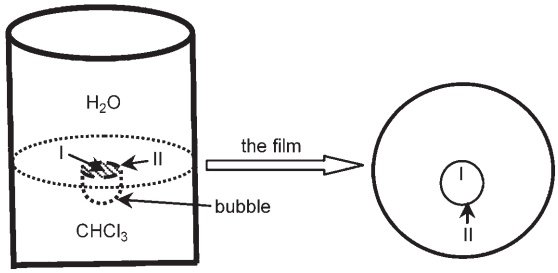

Figure 6. Diagram showing the process leading to formation of the flowerlike microstructure.

The fluorescence spectrum of the film shown in Figure 7a exhibits different features from that of monomeric porphyrin. Band I at 646 nm and band II at 713 nm in the fluorescence spectrum of monomeric TPyP correspond to the emissions from the excited singlet state S_1 to the basic state S_0, which arise from the excitation $\alpha_{2u}(\pi)$–$e_g(\pi^*)$.[13] They are mirror symmetric to the absorption Q-bands.[14,15] Whereas three fluorescence bands at 656, 685, and 721 nm occur in film II, they are redshifted in comparison with monomeric TPyP. Correspondingly, the absorption Soret band splits into two bands at 419 and 451 nm and is redshifted in comparison with that of the monomeric porphyrin at 412 nm (Figure 7b). Generally, there are side-by-side J-aggregates and face-to-face H-aggregates in porphyrin aggregation modes. The redshift and the splitting of the Soret band indicate that porphyrin molecules are in the J-aggregate mode in the composite.[16] The aggregation makes orderly stacks of porphyrin molecules, which results in larger Coulombic interaction energies and smaller band gaps; this induces the redshifts in the emission bands.[17] A similar phenomenon existed in film I.

Because the composite film is formed at the $H_2O/CHCl_3$ interface, each surface of the film (towards the H_2O or the $CHCl_3$ phases) has different nanostructures and distinct soakage properties. Film I-W is composed of straight-standing prisms, and the air fills in the space between the prisms.

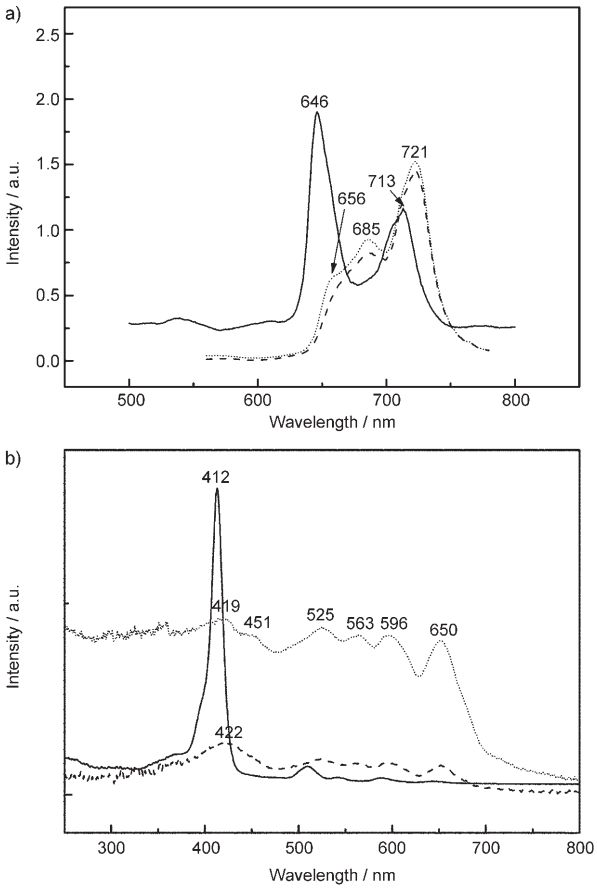

Figure 7. a) Fluorescence and b) UV/Vis spectra of the obtained films (film I (-----), film II (•••••), and monomeric TPyP (——)).

The inhomogeneous height of the prisms induced a dynamic soaking process. The contact angle of film I-W changed from approximately 130 to approximately 80° in 30 s (Figure 8a). Film I-O with a hierarchical micro- and nanostructure is superhydrophobic initially, but the contact angle gradually changes from approximately 150 to approximately 120° (Figure 8b). This might be attributed to a slow release of the air absorbed in the complex structure. The inhomogeneous hierarchical structure in film I-O induces and promotes the air-releasing process (Figure 1c). Whereas the microtextures in film II-O are more uniform and compact (Figure 5b), which give it superhydrophobicity with the stable contact angle 152.1° (see Figure S2a in the Supporting Information). Furthermore, a high-sensitivity micro-electrome-

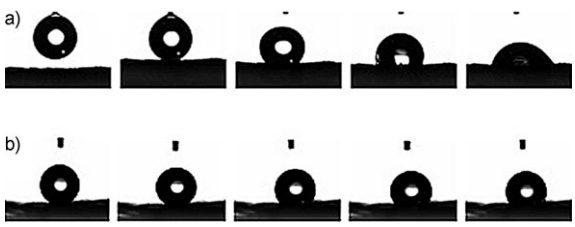

Figure 8. Soakage properties of a) film I-W, and b) film I-O.

chanical balance system was used to measure the force required to take a water droplet away from superhydrophobic film II-O. This force can be regarded as the adhesive force between film II-O and water. The corresponding force/distance curve recorded in Figure S2b in the Supporting Information, shows the corresponding maximum adhesive force is 66.3 μN, which is higher than that for the reported polystyrene nanotube arrays (59.8 μN).[18]

Conclusion

We reported a facile method for fabricating two rare distinct hierarchical organic nanostructures on the two sides of a supramolecular film for the first time, by using hydrogen-bonding interactions between tetrapyridylporphyrin and benzene-1,3,5-tricarboxylic acid at the H_2O–$CHCl_3$ interface. The surface of the film facing water is composed of nanoprism arrays, whereas the surface facing towards $CHCl_3$ is composed of three-dimensional sunflower-like hierarchical micro- and nanostructures. Each side of the film exhibits distinct soakage properties. We found FTIR spectral evidence that all pyridyl groups of TPyP hydrogen bonded to the carboxylic acid groups of BTC. The aggregation modes of porphyrin presented in this supramolecular film were studied by UV/Vis and fluorescence spectroscopy. This method can be extended to prepare other organic functional nanomaterials and fabricate advanced architectures of organic nanostructures.

Experimental Section

General remarks: FTIR spectra were recorded on a Bruker Vector 22 FTIR spectrophotometer at a resolution of 2 cm^{-1} in KBr disks (Bruker, Sweden). NMR spectra were collected on AVANCE DAX-500 500 MHz superconducting NMR spectrometers (Bruker, Sweden). UV/Vis absorption spectra of the samples dispersed in ethanol were conducted on a UV3100-NIR-Recording spectrophotometer operated at a resolution of 2 nm (Shimazu, Japan). Fluorescence (FL) spectra were measured on an AB2 fluorescence spectrometer at a power of 800 W (SLM, America). SEM images were taken on a JEOL JSM-5610 LV scanning electron microscope, and JEO-1500 VP field emission scanning electron microscope. Water contact angles were measured on a Data-Physics OCA 20 contact angle system at ambient temperature.

Measurement of the maximum adhesive force of the film: The force required to take the water droplet away from the hydrophobic surface was measured by using a high-sensitivity micro-electromechanical balance system (Data-physics OCAT 11, Germany). Firstly, a 3 mg water droplet was suspended within a metal ring, and film II-O was placed on the balance table. The film was moved upward at a constant speed of 0.01 $mm\,s^{-1}$ until it came in contact with the water droplet (process 1). Then, the film was moved down at a constant speed of 0.01 $mm\,s^{-1}$. The force increased gradually until it reached the maximum, subsequently the shape of the droplet changed from spherical to elliptical (process 2). When the film was moved down further, the film II-O broke away from the water droplet, the adhesive force decreased to zero immediately to finish one cycle of the force measurement (process 3). The force that the water droplet was subjected to could be regarded as the adhesive force between film II-O and water. The maximum force was about 66.3 μN (however if water remains on the film surface, the measurement cycle cannot be completed).

Acknowledgements

Financial support from the National Natural Science Foundation of China (project nos. 90606005, 20490210, 20371026, and 20571040) is greatly appreciated. The authors are grateful for the generous help with the characterization of wettability from Dr. X.F. Gao at the Institute of Chemistry, Chinese Academy of Sciences and National Center for Nanoscience and Technology in (P.R. China).

[1] A.-M. Cao, J.-S. Hu, H.-P. Liang, L.-J. Wan, *Angew. Chem. 117*, **2005**, 4465–4469; *Angew. Chem. Int. Ed.* **2005**, *44*, 4391–4395.
[2] G. M. Whitesides, B. Grzybowski, *Science* **2002**, *295*, 2418–2421.
[3] Z. L. Wang, *Adv. Mater.* **1998**, *10*, 13–30.
[4] M. Li, H. Schnablegger, S. Mann, *Nature* **1999**, *402*, 393–395.
[5] Z. P. Zhang, H. P. Sun, X. Q. Shao, D. F. Li, H. D. Yu, M. Y. Han, *Adv. Mater.* **2005**, *17*, 42–47.
[6] S. Takahashi, H. Miura, H. Kasai, S. Okada, H. Oikawa, H. Nakanishi, *J. Am. Chem. Soc.* **2002**, *124*, 10944–10945.
[7] A. D. Peng, D.-B. Xiao, Y. Ma, W.-S. Yang, J.-N. Yao, *Adv. Mater.* **2005**, *17*, 2070–2073.
[8] H. B. Fu, D. B. Xiao, J. N. Yao, G. Q. Yang, *Angew. Chem.* **2003**, *115*, 2989–2992; *Angew. Chem. Int. Ed.* **2003**, *42*, 2883–2886.
[9] X. J. Zhang, X. H. Zhang, K. Zou, C.-S. Lee, S.-T. Lee, *J. Am. Chem. Soc.* **2007**, *129*, 3527–3532.
[10] A. D. Adler, F. R. Longo, J. D. Finarelli, J. Goldmacher, J. Assour, and L. Korsakoff, *J. Org. Chem.* **1967**, *32*, 476.
[11] D. Q. Li, B. I. Swanson, J. M. Robinson, M. A. Hoffbauer, *J. Am. Chem. Soc.* **1993**, *115*, 6975–6980.
[12] S. L. Johnson, K. A. Rumon, *J. Phys. Chem.* **1965**, *69*, 74–86.
[13] Y. Y. Shi, W. Q. Zheng, X. Q. Li, L. X. Yu, X. Q. Wang, *Chin. Uni. Chem. Lett.* **2005**, *26*, 9–12.
[14] D.-J. Qian, A. Planner, J. Miyake, D. Frackowiak, *J. Photochem. Photobiol. A* **2001**, *144*, 93–99.
[15] B.-K. An, S.-K. Kwon, S.-D. Jung, S. Y. Park, *J. Am. Chem. Soc.* **2002**, *124*, 14410–14415.
[16] T. Yamaguchi, T. Kimura, H. Matsuda, T. Aida, *Angew. Chem.* **2004**, *116*, 6510–6515; *Angew. Chem. Int. Ed.* **2004**, *43*, 6350–6355.
[17] Y. S. Zhao, W. S. Yang, D. B. Xiao, X. H. Sheng, X. Yang, Z. G. Shuai, Y. Luo, J. N. Yao, *Chem. Mater.* **2005**, *17*, 6430–6435.
[18] M. H. Jin, X. J. Feng, L. Feng, T. L. Sun, J. Zhai, T. J. Li, L. Jiang, *Adv. Mater.* **2005**, *17*, 1977–1981.

Received: December 25, 2007
Published online: May 28, 2008

